FIRE AND MATERIALS
Fire Mater. **22**, 221–237 (1998)

Gasification of Silicone Fluids Under External Thermal Radiation Part I. Gasification Rate and Global Heat of Gasification†

Philip J. Austin,‡ Robert R. Buch*,§ and Takashi Kashiwagi
Building and Fire Research Laboratory, National Institute of Standards and Technology, Gaithersburg, MD 20899, USA

Transient gasification rates and fluid temperatures were measured for polydimethylsiloxane fluids ranging in viscosity from 0.65 cS to 60 000 cS in a nitrogen atmosphere at external radiant fluxes from 20 kW/m² to 70 kW/m². A detailed energy balance for each fluid sample was conducted to determine its global heat of vaporization. Two major energy loss corrections were identified and quantified. The absorption of incident radiation by the volatile products from short chain oligomers was measured and found to substantially reduce the incident flux to the sample surface; the energy loss due to re-radiation was determined to be a substantial factor in reducing the net heat flux to the sample for long chain length fluids. Other energy losses, e.g. heat loss to the substrate, were observed but were less significant. The average gasification rate for each fluid increased linearly with increasing external radiant flux. The global heat of gasification increases with an increase in the chain length (molecular weight) for the siloxane oligomers. These agreed well with calculated values. The global heat of gasification for 50 cS fluid is about 1200 kJ/kg and its value remains nearly constant for all higher molecular weight dimethylsiloxanes. Pyrolysis rates for siloxane fluids are very sensitive to trace catalysts. Measurements of the global heat of gasification for ultra-clean polymers resulted in significantly higher values (3000 kJ/kg). The gasification of siloxanes occurs via two modes or combinations thereof: (1) volatilization of molecular species native to the polymer, and (2) volatilization of thermal degradation products. The former process dominates for low molecular weight siloxanes ($\eta < 10$ cS) and the latter process dominates for high molecular weight siloxanes ($\eta > 1000$ cS). For the intermediate molecular weight siloxanes, both volatilization and degradation processes occur. © 1998 John Wiley & Sons, Ltd.

INTRODUCTION

Since their discovery in the 1930s and subsequent development during the past fifty years, silicones have grown into a multi-billion dollar industry. Silicones encompass a wide variety of novel materials that find applications in virtually every major industry sector ranging from cosmetics to electronics to defense/aerospace to automotive. Silicones offer an alternative to 'organics' in certain applications; new potential applications include their use as precision cleaning solvents, fire resistant communication cable components, fire retardant additives for thermoplastics, and other fire-related applications. The dominant polymer in the silicone industry is polydimethylsiloxane (PDMS) which has a backbone structure consisting of repeating siloxane units (alternate silicon and oxygen atoms); typically, the silicon atom has methyl substituents.

The polymers consist of a distribution of trimethylsiloxy end-blocked species, $(CH_3)_3Si–O[Si(CH_3)_2–O]_n–Si(CH_3)_3$, where n indicates average degree of polymerization, i.e. the number of siloxane monomer units in the molecule.¶ Incorporation of appropriate functional backbone substituents or chain end-groups provides a variety of cure chemistries for formulating a broad range of product forms (coatings, gels, foams, sealants, rubbers).

In addition to their unique surface, physical, and chemical properties, several current applications of these materials, e.g. dielectric coolants, firestop foams, rely to a large extent on the unique fire properties of silicones. The combustion of long chain PDMS exhibits a low heat release rate and the unique characteristic that the heat release rate does not increase significantly with an increase in external applied thermal radiant flux[1] or pool size;[2–4] these burn characteristics are intrinsic to dimethyl substituted siloxanes. This is in sharp contrast to most hydrocarbon materials whose heat release rates

*Correspondence to Robert R. Buch, Dow Corning Corporation, 2200 w.salzburg Rd., Auburn, MI 48611.
†Contribution from the National Institute of Standards and Technology. This paper was written under the auspices of the US Government and is therefore not subject to copyright in the US.
‡Present address: Acorn Industries Inc., 11844 Brookfield Avenue, Livonia, MI 48150, USA.
§Research associate from Dow Corning Corporation, Auburn, Michigan 48611, USA.
¶A convenient shorthand notation for PDMS polymers is: MD_nM (linear structures) and D_n (cyclic structures) where $M = (CH_3)_3SiO_{1/2}$, $D = (CH_3)_2SiO_{2/2}$, and n is the chain length for pure oligomeric cyclics or linears and n is the *average* chain length for polydisperse polymers. Other structural siloxane units are represented by: $T = (CH_3)SiO_{3/2}$, and $Q = SiO_{4/2}$. All commerically available oligomer/homopolymer silicones from the shortest chain length (MM) to the long chain polymers are fluids (due to the exceptional flexibility of the Si–O–Si bond). In the silicone industry, these polymers are typically referred to by their viscosity (η) in centistokes [cS], which is directly related to n (See Table 1) and their molecular weight.

CCC 0308–0501/98/060221–17$17.50

Received 4 April 1998
Accepted 28 September 1998

increase substantially with an increase in external thermal radiant flux.[1] The burning rates of large pool fires of PDMS are much lower than hydrocarbons. One of the causes of the lower burning rate is attributed to the accumulation of the silica ash layer at the silicone fuel surface.[2,3] This accumulation of amorphous silica ash at the surface results from the deposition of silica particles — a major combustion product of silicone oligomers (cyclic and or linear structures) in the gas phase.

Early studies by Lipowitz *et al.* resulted in a proposed model for the combustion of these materials.[6,7] Insight into the burning behavior of polydimethylsiloxane (PDMS) is evident from the complete combustion stoichiometry:

$$(CH_3)_3Si\text{–}O[\text{–}Si(CH_3)_2\text{–}O]_n\text{–}Si(CH_3)_3 + (12 + 4n)O_2 \rightarrow (2 + n)SiO_2 + (6 + 2n)CO_2 + (9 + 3n)H_2O$$

$$\Delta H_{comb}(\text{Gross}) = 26.5\ \text{MJ/kg}$$

$$\Delta H_{comb}(\text{Net}) = 24.8\ \text{MJ/kg}$$

where, for example, the combustion of 1 mole of MD_1M leads to the formation of 3 moles of SiO_2, an amorphous, white particulate ash. The deposition rate of silica on to the fuel surface increases with an increase in PDMS chain length[1,5] for low viscosity fluids and reaches a limiting rate at fluid viscosities of approximately 50 cS. In contrast to longer chain silicones, the burning rate of short chain cyclic and linear oligomers increases significantly with an increase in external thermal radiant flux and no significant accumulation of silica ash layer at the fuel surface is observed for these materials.[1,5] Removal of the particulate silica results from the fire plume buoyancy, i.e. high mass vaporization rate of the fuel and strong convective combustion product flow rates.

The fire behavior (ease of ignition, heat release rate) of a material results from the gasification processes which occur as a result of the thermal energy imposed on the material. An understanding of the gasification processes, i.e. the dominant mechanisms, energy requirements, and ensuing volatile products, is relevant and perhaps essential for modeling systems in which these materials are used. For short chain length PDMS fluids, it is expected that vaporization will be the dominant gasification process because of their low boiling temperatures (high vapor pressure) and relatively low heats of vaporization. Intermediate viscosity PDMS fluids consist of a broad distribution of different chain length components: short chain length species will vaporize while longer chain length components may thermally decompose resulting in the formation of cyclic oligomers. Gasification of high viscosity fluids perhaps occurs almost exclusively via thermal degradation to volatile cyclic oligomers.[8–11] Since the gasification of PDMS fluids under fire conditions may involve several gasification mechanisms, the global heat of gasification of PDMS may depend strongly on the composition of the fluid, i.e. the distribution of structures and their respective molecular sizes or chain lengths.

It is of interest to understand the gasification process of PDMS for a wide range of fluids exposed to external thermal radiant fluxes relevant to fire. Limited data are available on the global heat of gasification of PDMS. Two previous studies measured the gasification rate of 50 cS PDMS in nitrogen or reduced oxygen (volume fraction of 7%) atmospheres under various external radiant fluxes.[2,4] A small increase in the gasification rate with an increase in external radiant flux was observed from 26 kW/m^2 up to 56 kW/m^2 in a 7%(v/v) oxygen atmosphere[2] and up to 37 kW/m^2 in nitrogen.[4] At higher fluxes, the rate of increase of the gasification rate increased substantially. It was speculated that there were two regimes of gasification, perhaps the result of different thermal decomposition mechanisms and rates. Subsequent to these earliest studies, Steciak and Tewarson[12] measured a range of key fire parameters for both organic and silicone dielectric fluids and several resin compounds. A unique apparatus and novel approach was developed to eliminate the influence of the silica ash layer on the gasification behavior of the silicone fluid. The 'dual regime' gasification behavior of silicone fluid was again observed and heats of gasification were reported for the respective regimes (1800 kJ/kg and 3900 kJ/kg).

To understand the gasification processes of PDMS under conditions similar to those in fires, a wide range of PDMS fluids (0.65 cS to 60 000 cS) were exposed to various external radiant fluxes, up to 70 kW/m^2 in a nitrogen atmosphere. Gasification rates and fluid temperatures were measured. Since oxygen cannot reach the gasifying fluid surface in a pool burning configuration due to highly efficient oxygen-consuming gas phase oxidation reactions, a nitrogen atmosphere was used to avoid any oxidative degradation. Extensive characterization data on the gasification products are reported in Part 2 of this investigation.[13]

EXPERIMENTAL APPARATUS

Materials

The fluids used in this investigation were commercial-grade materials supplied by Dow Corning Corporation.‡ The fluids studied were octamethylcyclotetrasiloxane $[(CH_3)_2SiO]_4$, and a series of trimethylsiloxy end-blocked polydimethylsiloxane (PDMS) fluids, $(CH_3)_3Si\text{–}O[\text{–}Si(CH_3)_2\text{–}O]_n\text{–}Si(CH_3)_3$. In Table 1, the molecular structural description and molecular weight of each fluid are given along with relevant thermochemical property data.

Gasification apparatus

For these experiments, a radiant gasification apparatus, somewhat similar in design to a cone calorimeter, was constructed. The primary difference between the gasification apparatus and a typical cone calorimeter is that, in

‡ Certain trade names and company products are mentioned in the text or identified in an illustration in order to specify adequately the experimental procedure and equipment used. In no case does such identification imply recommendation or endorsement by NIST, nor does it imply that the products are necessarily the best available for this purpose.

Table1. Fluid-polymer properties[14]

Fluid/cS	Composition[a]	MW	BP (°C)	Q (kJ/kg)	H_V (kJ/kg)	G_f (kJ/kg)[b]
0.65	MD_0M	162	100	158	193	351
1.0	MD_1M	237	153	250	153	403
1.5	MD_2M	311	194	324	130	454
2.0	MD_3M	385	230	391	115	506
	D_3	222	135		160	
2.3	D_4	296	176	286	130	416
	D_5	370	211		113	
	D_6	444	245		101	
	D_7	518	276		92	
	D_8	592	303		84	
	D_9	666	326		79	
	MD_4M	459	260	447	104	550
	MD_5M	533	287	494	96	590
	MD_6M	607	311	547	89	636
	MD_7M	681	334	589	83	672
	MD_8M	755	355	635	77	712
5	MD_8M		(3)			
10	$MD_{15}M$		(3)			
20	$MD_{28}M$		~375[d]			~3000[e]
50	$MD_{58}M$		~375[d]			~3000[e]

[a] $M=(CH_3)_3SiO_{1/2}$, $D=(CH_3)_2SiO$.
[b] $G_f=\Delta H_V+Q$, where $Q=\int c_p(T)\,dT$, and ΔH_V is the heat of vaporization at BP.
[c] Does not exhibit a characteristic boiling point.
[d] Approximate onset temperature for thermal degradation (reversion) to volatile cyclics (D_3, D_4, ..., D_n).
[e] $G_f=\Delta H_{DEP'N}+Q$, where $Q=\int c_p(T)\,dT$, and $\Delta H_{DEP'N} \approx 180$ to 335 kJ/mole.

the gasification apparatus, the radiant exposure of the sample occurs in a sealed cylindrical chamber which is continuously purged with a controlled gas mixture typically nitrogen, rather than in the open air. As a result, the gasification apparatus was designed for studying the gasification processes of polymeric samples by measuring mass loss rate and temperatures of the sample rather than for calorimetry. A drawing of the gasification apparatus is provided in Fig. 1 and a detailed description of the apparatus in given elsewhere.[15] The apparatus consists of a stainless-steel cylindrical chamber that is 1.70 m tall and 0.61 m in diameter. In order to maintain a negligible background heat flux, the interior walls of the chamber are painted black and the chamber walls are water-cooled to 25°C. Purge gases are introduced into the chamber via an annulus at the bottom of the chamber.

A 30 cm diameter cone-shaped heater, which contains three coiled elements, is considerably larger than that used in a typical cone calorimeter which has a single coiled element. Its design allows for a more uniform planar heat flux distribution over a wide range of distances from the heater. The sample is positioned under the center of the heater using a block of Foamglas® insulation on which the sample or a dish containing the sample (for liquids), is placed. The incident flux to the sample is controlled by adjusting the distance between the sample and the heater which is held at a constant temperature of 750°C. With this procedure, the incident flux has the same spectral distribution at all flux levels. Heat flux measurements using a 16 mm diameter Gardon-type gauge showed the minimum flux at the edge of a 10 cm diameter circle to be within 91% of the centerline flux for the full range of incident flux exposures (20–70 kW/m^2).

The gasification apparatus is equipped with a retractable water-cooled shutter positioned to shield the sample

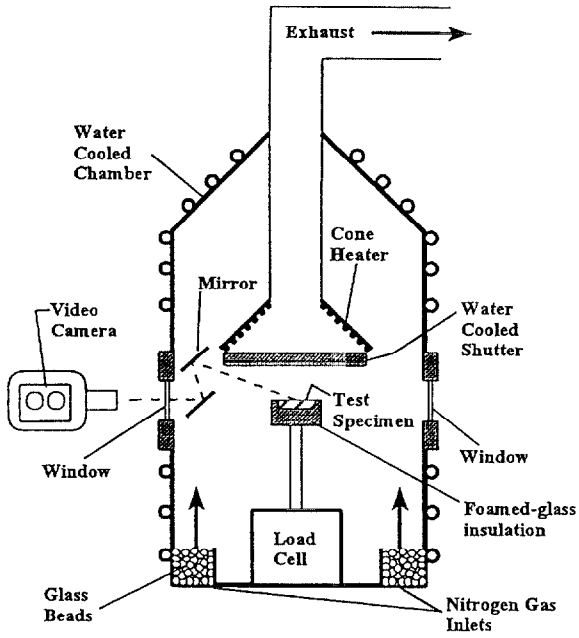

Figure 1. Schematic illustration of the gasification apparatus.

from the heater flux. This shutter is held in place prior to each test and retracted to begin the test. The chamber's base plate is connected to a hydraulic lifting mechanism which allows it to be lowered from the bottom of the chamber. Two optical ports on the sides of the chamber, just beneath the level of the heater, allow observation of the sample during testing. In addition, a periscope-like system of mirrors is used at one of the optical ports to

allow viewing of the sample's top surface during gasification.

Sample holder

The PDMS fluids were contained in a dish that snugly rested in a cavity (10 cm × 1.5 cm) in the top surface of the Foamglas.® The bottom of this cavity was instrumented with a single 0.076 mm diameter type K thermocouple to monitor the temperature beneath the dish.

Several different dishes, each having unique characteristics, were used to hold the fluids in this study. Preliminary tests were conducted using specially made lightweight borosilicate glass dishes. Borosilicate glass was chosen because it could be fashioned to support thermocouples inside the fluid containing region of the dish. In addition, borosilicate glass is essentially a non-reactive material with beneficial thermal properties: high melting temperature, low thermal conductivity, and modest thermal mass. Trace alkali (sodium) on the glass surface was a concern insofar as providing a rearrangement catalyst; however, the dish surface was demonstrated to be chemically passive after two gasification experiments. The wall thickness of these dishes (0.5–0.7 mm) was about one-quarter of that found in commercial dishes. As a result, these dishes had considerably less thermal mass than a sample mass (typically about 100 g), and therefore had negligible influence on the test results.

A second dish (mass of 12 g) was instrumented with four thermocouples at heights of 3, 7, 14, and 20 mm above the dish's bottom. The thermocouples were suspended in the center of the dish at various heights by fusing them at points of entry in the sides of the dish. This dish was used to measure the transient temperature profile of the 1.5, 5, and 50 cS fluids for a range of fluxes between 30 and 60 kW/m^2.

Since the thin-walled borosilicate glass dishes were very fragile and extremely difficult to fashion, the majority of the mass loss rate tests were conducted in more durable stainless steel dishes designed to minimize their thermal influence on the fluid being tested. The use of 0.051 mm thick shim sheet stock for fabrication allowed this dish to have a mass of 7 g. Despite their higher thermal conductivity than borosilicate glass, it is believed that this higher thermal conductivity did not result in a significant increase in the heat loss from the fluid due to their extremely thin wall. A more detailed discussion of the effects of the dishes on gasification rate is given in reference.[15]

EXPERIMENTAL METHOD

Typically, 100 g of fluid was used for each experiment. For volatile fluids, extra fluid was added such that 100 g of fluid would be in the dish at the time the sample was exposed to the heat flux. Typically, these 100 g samples were about 16 mm thick; however, this thickness varied somewhat among the fluids tested due to their different densities. The chamber was purged with nitrogen at a rate of either 12 L/s (1500 SCFH) or 23 L/s (3000 SCFH) depending on the expected mass loss rate of the fluid sample. For the low viscosity fluids (0.65 to 5 cS) a purge rate of 23 L/s (3000 SCFH) was necessary to prevent excessive accumulation of fluid vapor inside the gasification chamber. For the higher viscosity fluids (50 cS and higher) the 23 L/s (3000 SCFH) purge rate was only necessary when the heat flux level was greater than 40 kW/m^2. More details on the experimental procedure are given elsewhere.[15]

RESULTS

Observations were made for more than 100 fluid samples exposed to fluxes ranging from 20 to 70 kW/m^2 in a nitrogen environment. Using the stainless steel dish, mass loss rate measurements were conducted for 0.65, 1.0, 1.5, 5, 50, 1000, 10 000, and 60 000 cS PDMS-200 fluids. Simultaneous measurements of the mass loss rate and temperature profile were made using a borosilicate glass dish (with mounted thermocouples) for 1.5, 5, and 50 cS fluids at fluxes ranging from 30 to 60 kW/m^2.

General observations

One of the unique characteristics associated with the combustion of PDMS fluids is the formation of silica ash.[1,7] Although some of this ash is transported away from the fluid, much of the silica settles onto the fluid surface, creating an insulating layer of ash. Since no silica was observed during any of these tests, it can be concluded that silica does not form as a result of volatilization or pyrolysis; the formation of silica is a result of the combustion process.

Similarly, it was observed that a gelatinous layer does not form on the surface of PDMS fluids in the absence of oxygen. To further explore this effect, several tests were conducted in a partially oxidizing environment. Tests conducted on a 10 000 cS fluid at a heat flux of 60 kW/m^2 in 8 volume % oxygen showed the formation of a thin gel layer on the surface of the 10 000 cS fluid. No gel layer was observed in a nitrogen atmosphere.

Mass loss rate and temperature measurements

Throughout this study, distinct differences were observed in the gasification behavior of the various fluids. Based on these observations, fluids can be grouped into three general categories according to similar properties and gasification patterns: low, intermediate, and high viscosity fluids.

Low viscosity fluids. The low viscosity fluids consist of the 0.65 to 5 cS PDMS-200 fluids. Also included in this category is D_4, a cyclic siloxane structure. Although the 0.65, 1.0, and 1.5 cS fluids were used in the majority of tests, the 2.0 cS and D_4 were also studied on a limited basis. A description of the composition of these fluids along with relevant property data is provided in Table 1.

These fluids (except for the 5 cS fluid) are essentially single component fluids, i.e. > 97% of a single siloxane

oligomer. Because of their vapor pressure, the gasification process for these fluids consisted solely of volatilization. Figure 2 shows the mass loss plot for a 0.65 cS fluid sample exposed to a heat flux of 70 W/m^2. These data are typical for the low viscosity fluids for the range of heat fluxes studied. An initial transient period (loss of the first 5 to 10 g of fluid) occurs in which the mass loss rate rapidly increases followed by a long period during which a gradual increase in the mass loss rate occurs. When ~ 30 g of fluid remains, a final transient period occurs in which the mass loss rate rapidly increases. This final surge was also observed with toluene and methanol and is believed to result from the heated bottom surface of the dish enhancing the boiling process.

In Fig. 3, the mass loss rate data for 0.65 cS fluid exposed to different heat fluxes are given as a function of the normalized mass. The majority of mass is lost in the period between the initial and final transients. This period (the quasi-steady-state domain between the normalized mass values of 0.9 and 0.4) was used in calculating the average mass loss rate for these fluids. Use of normalized mass facilitated graphic comparison of experimental data with widely different time scales. Although this averaging method biases the average in favor of the higher mass loss rates, the difference between the normalized average and a traditional time based average was typically less than 10%.

A typical temperature distribution plot for a 1.5 cS fluid sample exposed to a heat flux of 30 kW/m^2 is given in Fig. 4. The traces in the plot represent the temperature measured at different heights above the bottom of the dish as measured by 0.076 mm diameter Type-K thermocouples. Two thermocouples did not contact the fluid: the 'Firebrick' thermocouple contacted the bottom surface of the borosilicate glass dish and the '20 mm from bottom' thermocouple was positioned above the surface of the fluid to provide a temperature measurement of the vapor layer. For those thermocouples that were in contact with the fluid, an inflection occurs in each temperature curve as the fluid level recedes past each thermocouple. Each inflection corresponds to the boiling point of the fluid confirming that only volatilization is occurring. Similar results obtained at heat fluxes of 40, 50, and 57 kW/m^2 confirm that gasification occurs only via volatilization. The initial overshoot of the boiling temperature as the fluid level drops through the level of the thermocouple is due to 'in-depth absorption' in the fluid which results in slightly higher temperatures just below the fluid surface.

Intermediate viscosity fluids. The intermediate viscosity fluids consist of the 10, 50, and 100 cS PDMS-200 fluids. A description of the composition of these fluids is given in Table 1. Unlike the low viscosity fluids, the intermediate viscosity fluids consist of distributions of PDMS polymers. Their gasification is not characterized by a well-defined quasi-steady-state mass loss interval. In addition, their gasification behavior is strongly influenced by the magnitude of the heat flux to which they are exposed as noted in Fig. 5. At all heat flux levels, the mass loss rate increases rapidly at first and then increases at a slower rate. At fluxes above 45 kW/m^2, a significant increase in the mass loss rate then occurs further into the gasification process when about 1/2 to 2/3 of the fluid has been gasified. The point of this transition occurs further into the gasification process as the heat flux is increased.

Analysis of the volatiles indicated that a two-stage gasification process is occurring.[1,3,2,4] Initially, gasification of these fluids is dominated by volatilization in which the shorter chain PDMS molecules are preferentially distilled from the fluid. The later stages of gasification are dominated by pyrolysis of the remaining fluid, in which the molecular bonds of the remaining long chain PDMS molecules are rearranged, forming cyclic siloxane

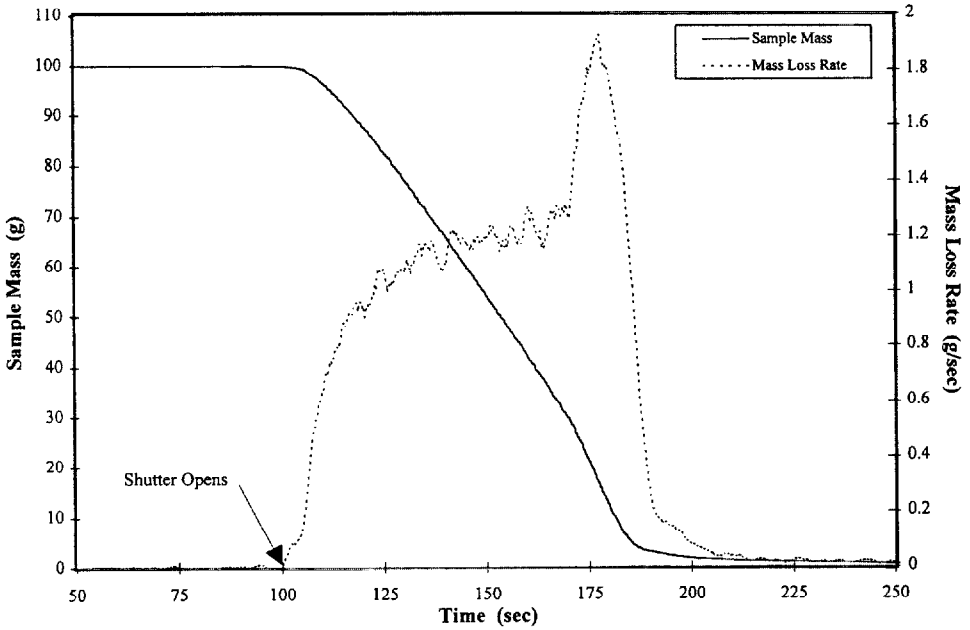

Figure 2. Sample mass and mass loss rate as a function of exposure time for 0.65 cS PDMS fluid exposed to a radiant flux of 70 kW/m^2.

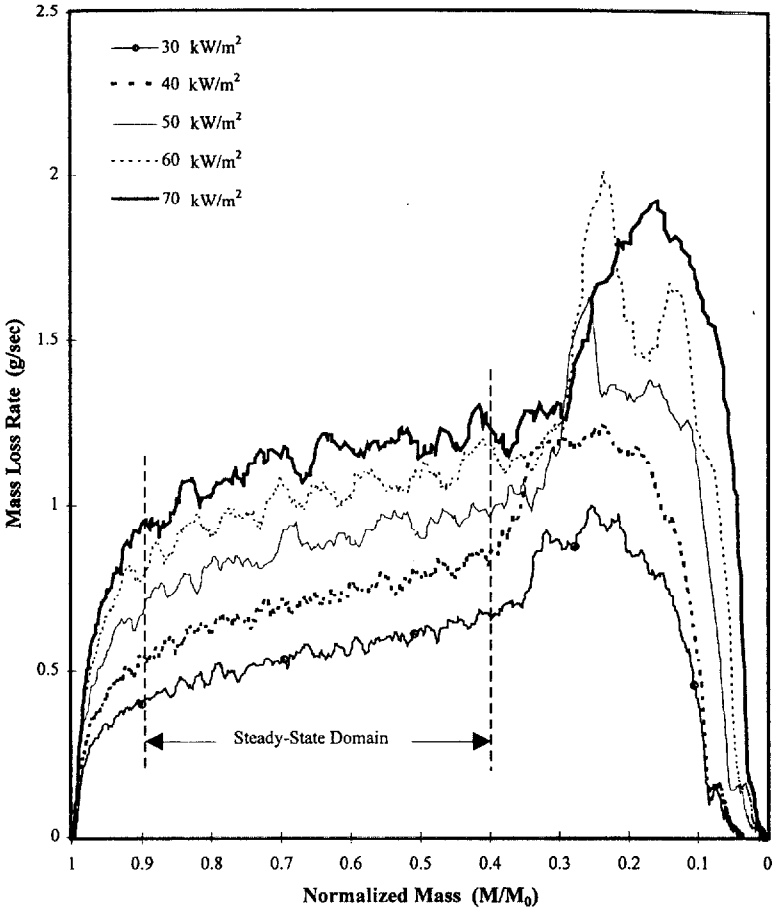

Figure 3. Sample mass loss rate as a function of normalized sample mass for 0.65 cS PDMS fluid exposed to different radiant fluxes.

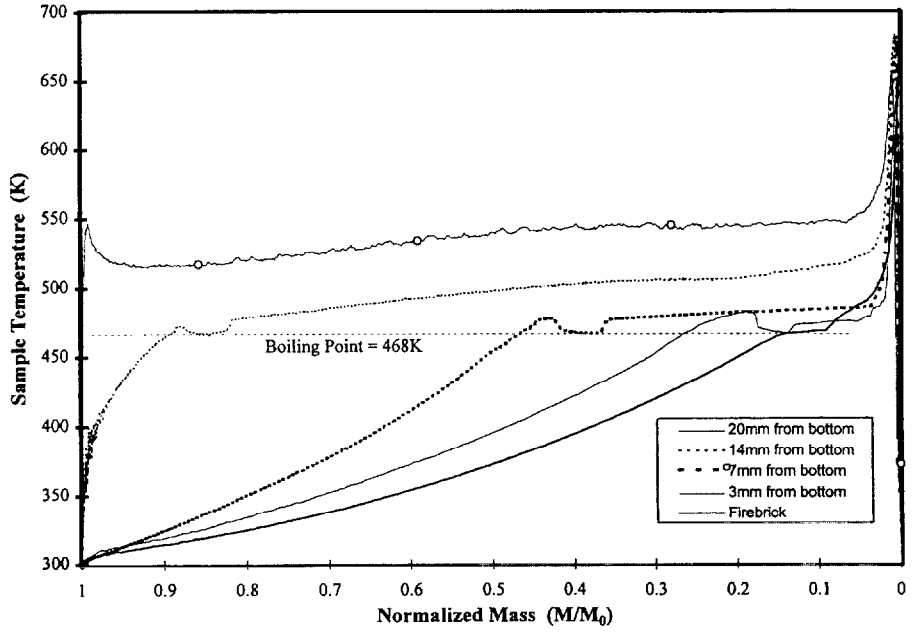

Figure 4. Sample temperatures at different distances from the bottom of the dish as a function of normalized mass for 1.5 cS PDMS fluid exposed to a radiant flux of 30 kW/m².

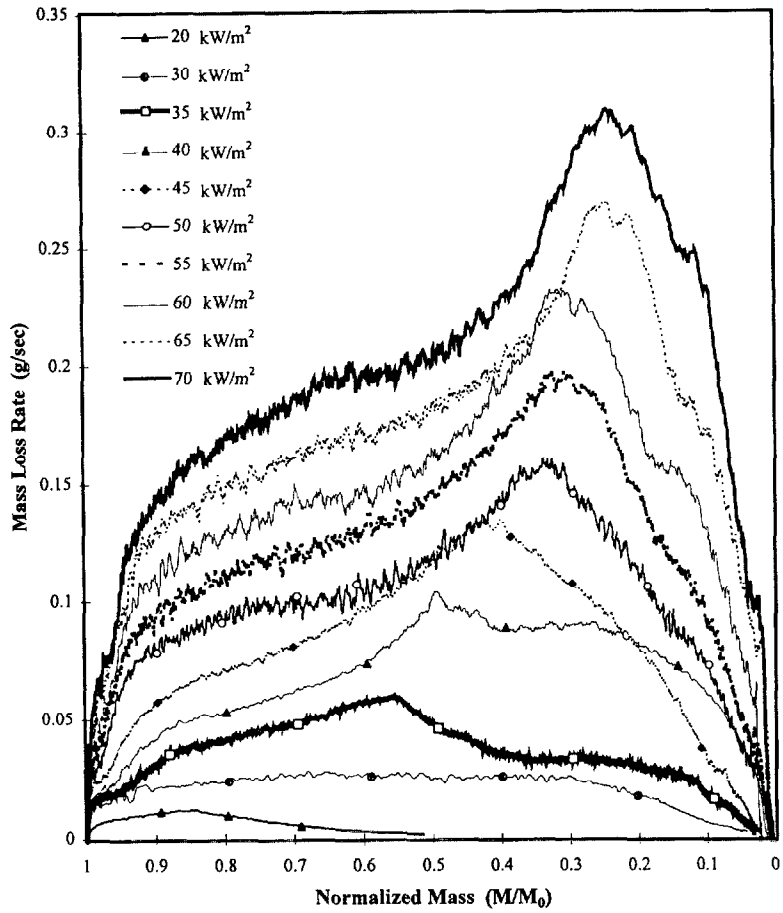

Figure 5. Sample mass loss rate as a function of normalized sample mass for 50 cS PDMS fluid exposed to different radiant fluxes.

molecules which are then vaporized. The transition between these two processes is governed by the temperature profile within the fluid, and hence the heating rate of the sample. Because a sample exposed to a lower heat flux heats more uniformly, the majority of its fluid volume attains pyrolysis temperatures earlier in the gasification process (on a mass basis) than a sample exposed to a higher heat flux. As a result, at lower fluxes significant pyrolysis occurs simultaneously with volatilization, producing a gradual transition between these two processes and causing the peak mass loss rate to occur earlier in the gasification process.

The average mass loss rates of the intermediate viscosity fluids were computed for the domain between the normalized mass values of 0.9 and 0.1. This domain included both the volatilization dominant and pyrolysis dominant stages of gasification in the average while omitting the initial and final transient periods. For these fluids, bubbling of the fluid surface was observed to occur early during the gasification process. This was followed by the inception of bubbles forming well beneath the fluid surface, which subsequently resulted in vigorous bubbling of the whole fluid. This behavior is consistent with the fact that distillation of shorter chain molecules throughout the fluid volume will produce superheated fluid that will form bubbles. More detailed discussion of bubbling and accumulation of vapor near the surface is given in reference.[15]

A temperature distribution plot as a function of normalized mass is given in Fig. 6 for a 50 cS sample exposed to a heat flux of 50 kW/m^2. The curves represent the temperature measured at different heights from the inner surface of the bottom of the dish. It should be noted that although the fluid expanded, the '20 mm from bottom' thermocouple remained above the fluid surface throughout the tests. As the surface of the fluid receded and approached the level of each thermocouple, the temperature would rise more rapidly. As the surface receded past each thermocouple, an increase in noise in the thermocouple signal would occur as the thermocouple encountered the bubbling surface and then pass into the vapor layer. The initial overshoot and subsequent drop in the temperature that was observed for the low viscosity fluids did not occur for these fluids perhaps because of the turbulence caused by vigorous bubbling at the fluid surface. The increase in noise in the thermocouple signal, however, was still distinct enough to allow for a rough measurement of the fluid height to be obtained at various stages of the gasification process. In Fig. 6, the fluid surface passes through the '14 mm from bottom' thermocouple at a normalized mass of about 0.8 and through the '7 mm from bottom' thermocouple at a normalized

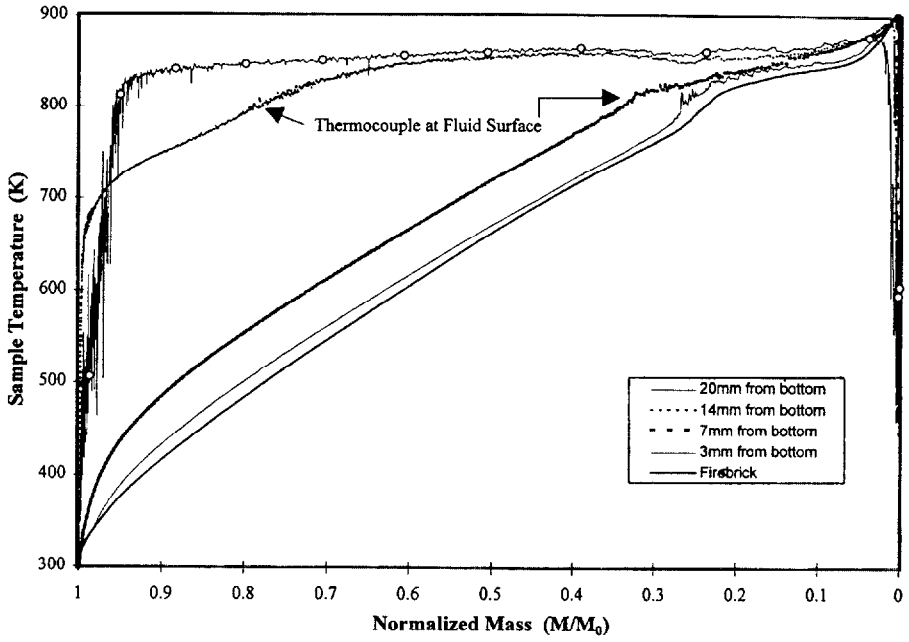

Figure 6. Sample temperatures at different distances from the bottom of the dish as a function of normalized mass for 50 cS PDMS fluid exposed to a radiant flux of 50 kW/m².

mass of about 0.35. One might similarly conclude from the plot that the fluid surface passes through the '3 mm from bottom' thermocouple at a normalized mass of about 0.3. Actually at this stage of the gasification process, the entire fluid volume is bubbling so vigorously that noise appears in the thermocouple signal even though the thermocouple is not yet at the surface of the fluid. One can observe from the plot that the fluid surface temperatures are well above those required for thermal induced degradation of PDMS molecules (> 650 K).

High viscosity fluids. A range of higher viscosity (10^3, 10^4, and 6×10^4 cS) fluids was investigated to provide insight into the dominant mechanisms occurring in polymers typically utilized in formulated products such as sealants, rubber, foams and gels. The analysis of volatile products and fluid residues[13] indicated the gasification process for these fluids consists primarily of thermal induced degradation to primarily short chain cyclic structures via siloxane rearrangement; however, significant volatilization occurs during the early stages of gasification. Like the intermediate viscosity fluids, these fluids are not characterized by a well defined quasi-steady-state mass loss period. For this reason, the average mass loss rates were calculated using the domain between the normalized mass values of 0.9 and 0.1. In addition, their pyrolysis is strongly influenced by the magnitude of the heat flux to which they are exposed. The pyrolysis data for 1000 cS fluid are given in Fig. 7. The mass loss rate increases with increasing heat flux and the maximum rate occurs at a lower value of the normalized mass as the heat flux increases. This shift in the mass loss peak is attributed to more uniform heating of the remaining sample at the lower heat flux exposures. At lower heat fluxes, the fluid volume attains pyrolysis temperatures earlier in the gasification process (on a mass basis). As a result, at lower heat fluxes pyrolysis transitions from a surface phenomenon to a volumetric process earlier in the gasification process, thus causing the peak mass loss rate to occur earlier.

The gasification behaviour of the high viscosity fluids resembled that of the 50 cS fluid in several respects. Their normalized average mass loss rates were roughly equivalent to that for the 50 cS fluid; however, peak mass loss rates were higher for the 50 cS fluid at a given flux. As they were heated, the high viscosity fluids' thermal expansion and bubbling behavior was similar to that observed for the intermediate viscosity fluids. For the 10 000 and 60 000 cS fluids, a notable difference in gasification behavior was observed at high heat fluxes (> 50 kW/m²). For these fluids, as the mass loss rate peaked at a normalized mass value of 0.5 or 0.4, the fluid would periodically expand due to intense bubbling, and then contract as the bubbles rapidly collapsed. This phenomenon was manifested as a periodic oscillation in the mass loss rate data as noted in Fig. 8. This behavior is perhaps attributable to thermal induced crosslinking (gel network formation) occurring in the fluid's upper surface because of the very high temperature in this region of the sample. This phenomenon will influence the gasification behavior of polymers more significantly as their initial viscosity (molecular size) increases.

Average mass loss rate

For the fluids studied in this investigation, the mass loss rate data fell into two data sets as given in Figs 9 and 10. For fluids which gasify via volatilization (Fig. 9), the average mass loss rate decreases as the viscosity (molecular size) of the volatile species increases. This behavior is consistent with the fact that as the chain length of the

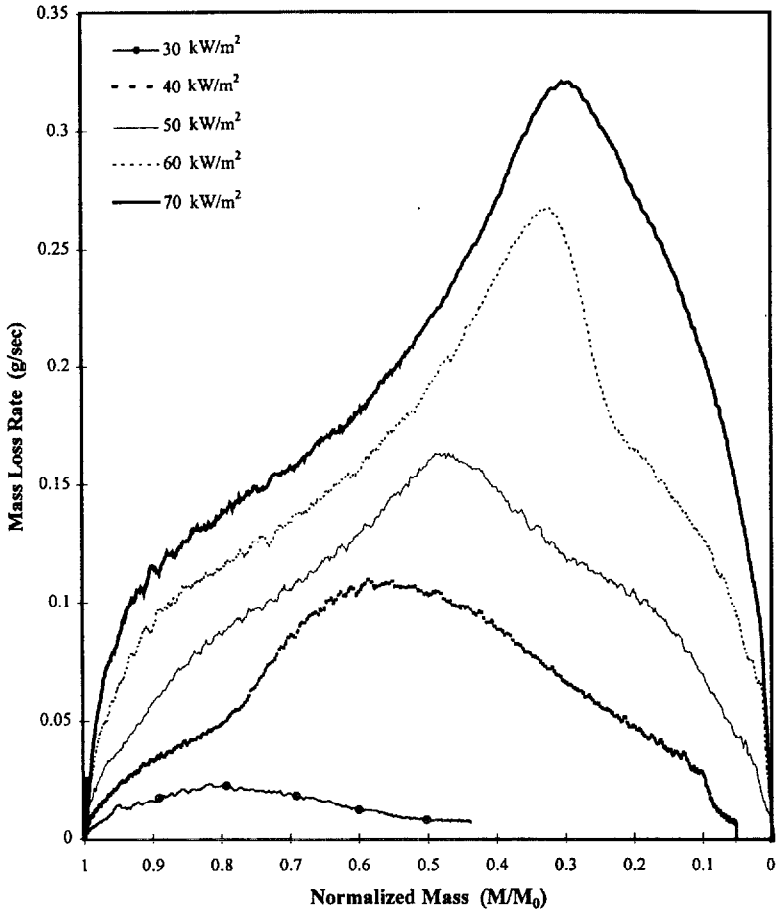

Figure 7. Sample mass loss rate as a function of normalized sample mass for 1000 cS PDMS fluid exposed to different radiant fluxes.

PDMS molecule is increased, more energy is required for it to heat to its boiling point and then vaporize (see Table 1). This energy required for gasification, commonly referred to as the global heat of gasification, will be discussed in detail in the next section of the paper. For fluids which gasify via thermal degradation and volatilization, the average mass loss rate is independent of the fluid viscosity (molecular size). Although some differences in the behavior of these fluids were observed, the gasification process for these fluids consists of two processes: early distillation of short chain molecules from the fluid mixture and thermal degradation of long chain molecules to form volatile cyclic siloxanes The result that these fluids have similar average mass loss rates appears to be an indication that both pyrolysis processes for these fluids require similar amounts of energy and the mass loss by distillation is less than that by pyrolysis.

Also noteworthy in both plots is the relatively linear relationship between the mass loss rate and heat flux. This linear relationship is of particular interest for the 50 cS fluid because previous studies[2,4] have indicated that a less regular relationship exists between these two parameters for this fluid. In these previous studies it was observed that a linear relationship exists between the mass loss rate and heat flux at low heat flux values; however, at a critical value of the heat flux, between 37 and 57 kW/m^2 depending on the study, the mass loss rate of the 50 cS fluid increases dramatically with further increases in the heat flux. From Fig. 10, it can be observed that no dramatic change in the mass loss rate was observed in this study for any of the fluids for the range of heat fluxes studied.

DISCUSSION

The global heat of gasification is a defined property of a substance that represents the amount of energy required to 'gasify' unit mass of the material. The global heat of gasification is defined mathematically as:

$$L = \frac{\dot{Q}''_{net}}{\dot{m}''}$$

where L is the global heat of gasification, $\dot{Q}''_{net}$ is the net heat flux to the sample, and $\dot{m}''$ is the mass loss rate per unit surface area. It is widely used in fire calculations to determine the amount of combustible gas that would be supplied to a fire when a material is exposed to a given heat flux. One of the primary goals of this investigation was to measure the global heat of gasification for the

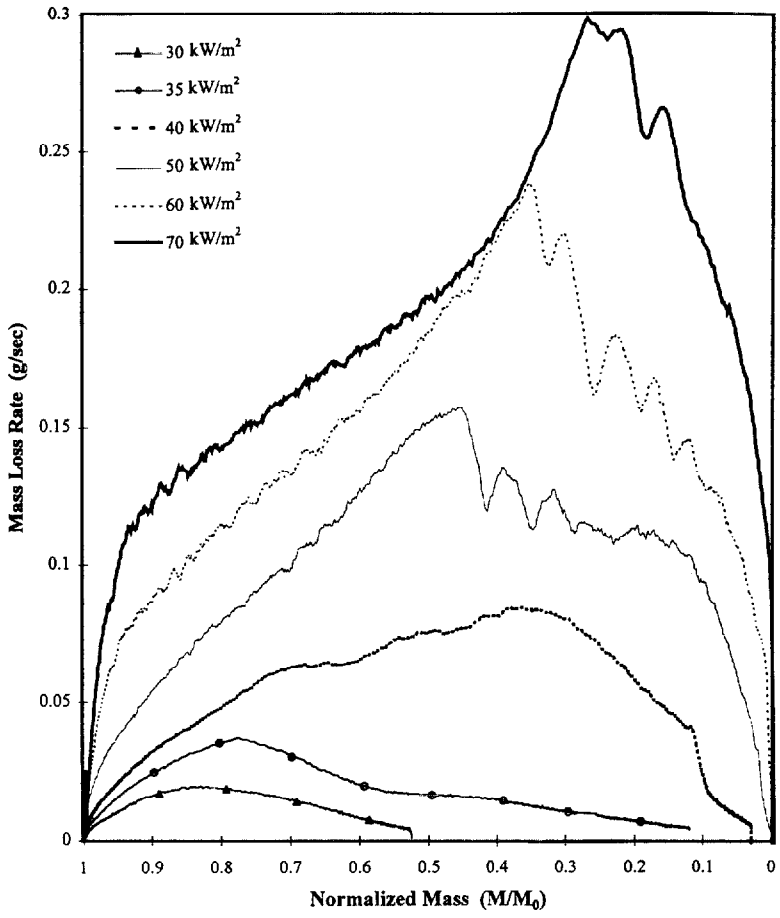

Figure 8. Sample mass loss rate as a function of normalized sample mass for 60 000 cS PDMS fluid exposed to different radiant fluxes.

PDMS fluids studied. Of particular interest, were the intermediate and high viscosity fluids, for which no consistent published values were available.

For pure materials that volatilize, this quantity simply represents the sum of the heat of vaporization and the sensible heat required to raise a unit mass of the material from ambient temperature to its boiling point. For materials that pyrolyze or mixtures of volatile materials, the definition of this property is not as clear. For these materials, the global heat of gasification can be highly dependent upon the conditions under which the material is gasified. Parameters such as heating rate and other environmental conditions can significantly influence the value of this property for such materials.

Typically, the global heat of gasification is measured and used as an average quantity. However, as Kashiwagi *et al.*[16] have shown, the instantaneous value of the global heat of gasification of any material, even solely volatilizing materials, varies with time for a given set of experimental conditions. To demonstrate this, one must first understand how the global heat of gasification is calculated from experimental measurements. Initially, as a material is heated, a large amount of the heating is dedicated to raising the temperature of the material rather than to gasifying it; therefore, the initial mass loss rate is low. This corresponds to a high instantaneous value of the global heat of gasification. As the material continues to heat, the mass loss rate eventually increases, and the corresponding value of the global heat of gasification decreases. Ideally, a steady-state will eventually be reached where the mass loss rate attains a steady or asymptotic value. This is the condition for which the global heat of gasification is typically reported. As can be seen, using this average value to estimate the mass loss rate during the initial stages of gasification may result in a significant over-estimation; therefore, care must be used in applying such average values of the global heat of gasification to a fire calculation if one does not account for the transient behavior of the gasification process.

According to Eqn (1), the quantities required for calculating the global heat of gasification are the mass loss rate and the net rate of heat transfer to the fluid. The latter requires an understanding of the energy balance for the sample which includes the incident radiant heat flux, the absorption of radiation by the vapor layer above the fluid, the absorption of radiation by the fluid or the transmission of radiation through it, the conduction of heat to the firebrick, the radiant re-emission by the fluid, and the convective cooling of the fluid surface by the nitrogen purge gas. For these experiments, the major factors in determining the net rate of heat transfer to the fluid were the incident flux, vapor absorption,

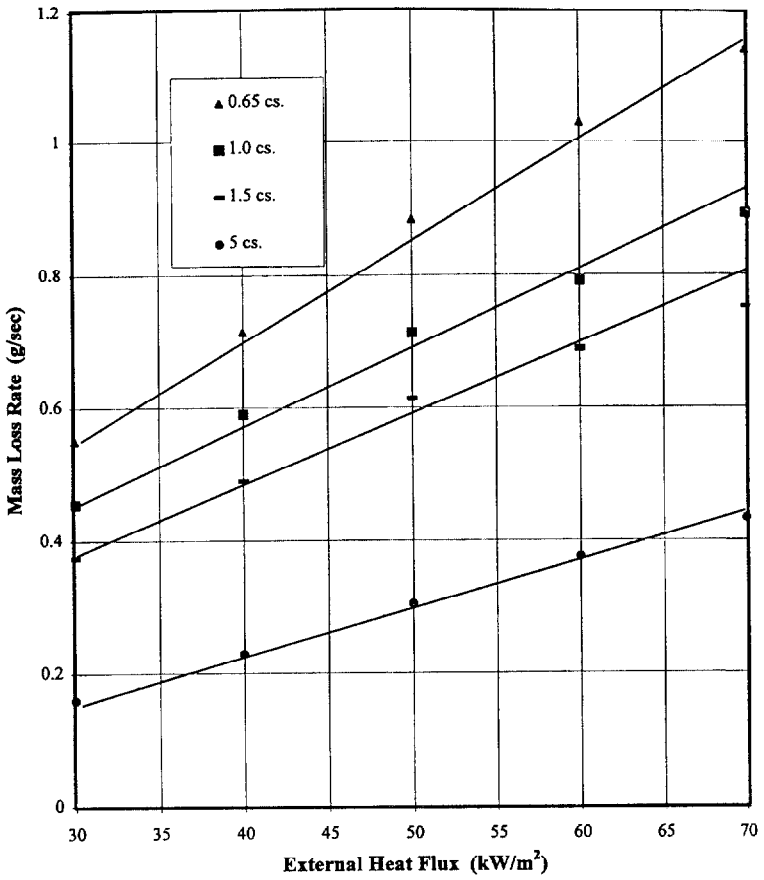

Figure 9. Average mass loss rate as a function of external radiant flux for short chain length PDMS fluids (0.65, 1.0, 1.5, 5 cS).

re-radiation, and to a lesser extent, convective cooling. The conduction of heat to the firebrick and radiant transmission through the fluid were minimal and not included in calculating the net heat transfer to the fluid.

Initially, the vapor layer was presumed to be only weakly absorbent and therefore was considered to have little effect on the net heat transfer to the surface. However, when initial attempts failed to reconcile the measured global heat of gasification values with the calculated values (based on heat capacity and heat of vaporization data) for these fluids, the validity of this assumption was tested. Preliminary tests conducted with 1.5 cS fluid showed that the vapor absorption effect was indeed substantial, absorbing up to 35% of the incident energy. This revelation prompted a more thorough investigation of this effect.

Vapor absorption fraction

A series of experiments were conducted to measure the vapor absorption fraction (heat flux absorbed by vapor layer/incident heat flux) for several PDMS fluids at several heat flux levels. The tests were conducted using a specially designed borosilicate glass dish that allowed simultaneous measurement of the vapor absorption effect and the mass loss rate. This dish was designed to simulate the experimental conditions of the standard mass loss rate experiments. The dish, which was configured like a donut, was fabricated from a standard borosilicate glass Petri dish and a segment of thin walled borosilicate glass tubing. The tubing, which protruded through the center of the dish, created a cylindrical hole inside which a heat flux gauge could be inserted. The top of the cylinder was positioned at a level of 8 mm below the lip of the dish in order to allow sufficient space for the vapor layer to form above the heat flux gauge. A detailed description of the sample holder and experimental procedure are given elsewhere.[15]

A composite heat flux plot of these tests for a 1.5 cS sample exposed to a heat flux of 40 kW/m^2 is given in Fig. 11. The magnitude of the vapor absorption effect is indicated by the difference between the 'heat flux with fluid' and the 'heat flux with window only' traces. Note the substantial reduction in heat flux level at the fuel surface after gasification commences. The continuous, slow, steady decrease in heat flux is due to the gradual mass loss rate increase; the heat flux reaches a minimum when the mass loss rate reaches its maximum. The initial rapid rise in mass loss rate does not produce an immediate large decrease in the heat flux. A probable explanation for this behavior is that the vapor layer has a maximum thickness and density for a given set of experimental conditions. This maximum thickness and

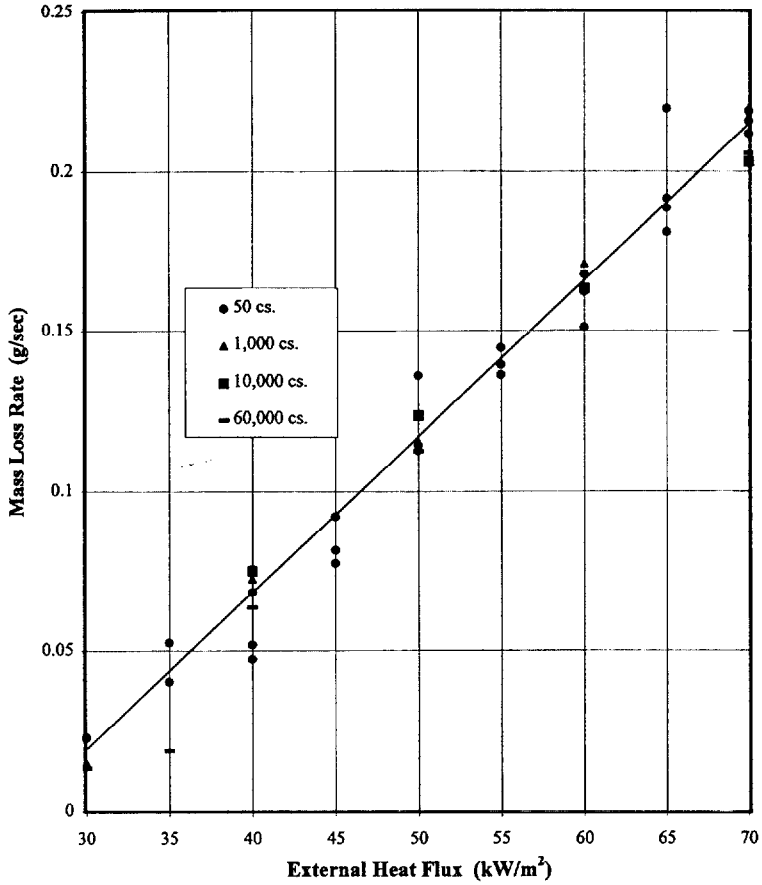

Figure 10. Average mass loss rate as a function of external radiant flux for long chain length PDMS fluids (50, 1000, 10 000, 60 000 cS).

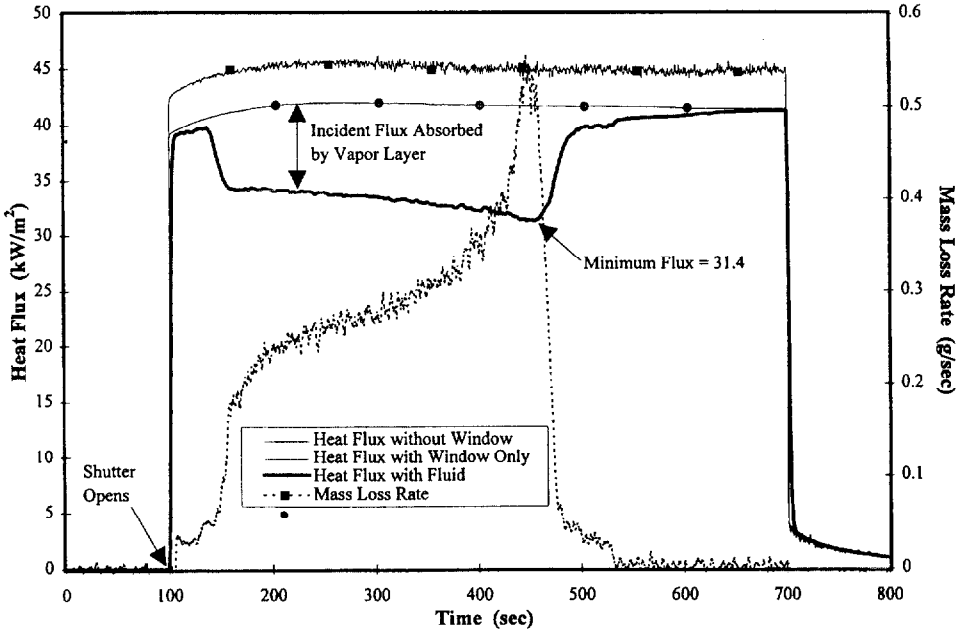

Figure 11. Measured radiant flux and mass loss rate as a function of exposure time for 1.5 cS PDMS fluid exposed to a radiant flux of 40 kW/m² in the 'vapour absorption dish'.

density is the result of the fluid dynamics dictated by the geometry of the dish, the mass loss rate, the properties of the vapor, and the flow field of the nitrogen purge gas.

Tests were conducted at heat fluxes of 40, 55, and 64 kW/m^2 for the 1.5, 5, and 50 cS fluids. Multiple tests conducted for each test condition showed reasonably repeatable results with respect to qualitative behavior but significant quantitative variability was observed in some cases. The tests revealed a strong relationship between the mass loss rate and the vapor absorption fraction at low mass loss rates. With the exception of the 50 cS fluid, at high mass loss rates the vapor absorption fraction was only weakly dependent on the mass loss rate. The tests also revealed a significant heat flux dependence of the results. This heat flux dependence is believed to be due to flow geometry changes related to the position of the sample dish with respect to the heater.

For the 1.5 cS fluid, it was observed that the vapor absorption fraction would increase steadily with increasing mass loss rate until it reached a value of the mass loss rate at which point the vapor absorption fraction would increase only slowly with further increases in the mass loss rate (Ref. 15 [Fig. 36]). The value of the mass loss rate at which this transitional behavior occurred increased with increasing heat flux. For the 55 and 64 kW/m^2 tests, the vapor absorption fraction increased to a value of between 0.25 and 0.30 at a mass loss rate of about 0.2 g/s, at which point the vapor absorption fraction held steady with further increases in the mass loss rate. For the 40 kW/m^2 case, the vapor absorption fraction rose to a value of 0.15 at a mass loss rate of 0.1 g/s, and then slowly increased to a value of 0.25 at a mass loss rate of 0.6 g/s. At all three heat flux conditions tested, the vapor absorption fraction had a relatively constant value of about 0.25 ± 0.05 for mass loss rates in excess of 0.4 g/s. The fact that at all three heat flux conditions the vapor absorption fraction attained a maximum asymptotic value is consistent with the explanation discussed above regarding the existence of a maximum vapor layer thickness. Because the average mass loss rates measured for the 1.5 cS fluid using the stainless steel dish were all near or above 0.4 g/s, a vapor absorption fraction of 0.25 was used for the purposes of calculating the global heat of gasification values. This vapor absorption value was also used for the calculations involving the 0.65 and 1.0 cS fluids.

The vapor absorption behavior of the 5 cS fluid (Ref. 15 [Fig. 37]) was observed to be similar to that of the 1.5 cS data at heat fluxes of 55 and 64 kW/m^2, i.e. the vapor absorption fraction would increase steadily with increasing mass loss rate until it reached an asymptotic value. At 40 kW/m^2, however, the vapor absorption effect never attains this asymptotic condition due to the lower mass loss rates. A reasonable estimate of 0.35 ± 0.05 for the vapor absorption fraction can be used at mass loss rate values above 0.18 g/s. For mass loss rates below 0.18 g/s, linear scaling was used to estimate the vapor absorption fraction. These estimates of the vapor absorption fraction were used in calculating the global heat of gasification values for the 5 cS fluid.

The absorption fraction for 50 cS fluid (Ref. 15 [Fig. 38]) was confined to a range of values bounded by two lines passing through the origin, one representing the maximum vapor absorption effect (at 40 kW/m^2) and the other representing the minimum (at 64 kW/m^2). At fluxes of 45 kW/m^2 and lower, the maximum vapor absorption fraction was used while at fluxes of 65 kW/m^2 and higher, the minimum vapor absorption fraction was used. For fluxes between 45 and 65 kW/m^2, the absorption fraction varied proportionately from the maximum to the minimum value. The error contribution to the heat of gasification associated with these estimates is believed to be $\pm$ 5%. The above correlation was used in the global heat of gasification calculations for the 50 cS fluid and the similar gasification behavior of the 50 cS and high viscosity fluids justified the use of this correlation for the 1000, 10 000 and 60 000 cS fluids. A detailed discussion and experimental data are given elsewhere.[15]

Re-radiation

Re-radiation from the surface of low viscosity fluids was not significant due to the low boiling temperatures of these fluids. Their re-radiation was estimated by assuming each fluid emitted as a gray body at its boiling temperature with an emissivity of 0.9.

For the high and intermediate viscosity fluids, re-radiation was substantial with values on the order of 1/3 of the incident heat flux. A method to estimate these re-radiation losses was developed.[15] Calculation of the re-radiation for these fluids was complicated by the fact that re-radiation occurs throughout the entire fluid layer. Therefore, to calculate the re-radiation by the entire fluid, each layer of fluid must be treated as a separate emitter. Calculation requires knowledge of the temperature as a function of depth within the fluid layer. In addition, the absorption coefficient of the fluid as a function of radiation frequency must be known in order to account for the attenuation of re-emitted energy by the surrounding fluid. Measurements of the absorbance as a function of frequency were made using a Fourier Transform Infrared Spectrometer (FTIR) that had a operating wavelength range of 2.3 to 13 mm. An adjustable thickness, sealed liquid cell with calcium fluoride windows was used for the measurements. Absorbance measurements were made for the operating range of the FTIR using 100 cS fluid samples having thicknesses of 0.5 and 0.1 mm. The absorbance data were then converted into values of the absorption coefficient. Because of the large path length used in these tests, these data were only useful in quantifying the absorption coefficient for the weakly absorbing frequency ranges. For the strongly absorbing ranges, estimates of the absorption coefficient were made from the published data and compiled with the above measured values. Using the absorption coefficient data and temperature data from the borosilicate glass dish tests, a computer model was used to calculate the re-radiation for the various experimental conditions. The model divided the fluid into thin layers that were each assumed to emit as blackbodies at their respective temperature. The amount of energy emitted by each layer, that was not absorbed by the fluid layers above it, was then calculated. The sum of the emitted energies from all of the layers provided the total re-emitted energy.

Re-radiation values were calculated for 5 and 50 cS fluids as a function of external heat flux and are given in Fig. 12. Re-radiation values ranged from 16 to 23 kW/m^2

for the 50 cS fluid and from 7.8 to 8.7 kW/m^2 for the 5 cS tests. The re-radiation values for 50 cS fluid were used in the global heat of gasification calculations for all high viscosity fluids.

Purge gas cooling

The nitrogen purge gas was tempered to ~ 30°C prior to entering the gasification unit. Nevertheless at low mass loss rates (< 0.05 g/s), nitrogen circulating above the sample surface caused convective cooling of the fluid. This effect was evidenced by the significantly lower fluid temperatures measured when the mass loss rate was less than 0.05 g/s, i.e. for high and intermediate viscosity fluids exposed to low heat fluxes (< 40 kW/m^2). A convective cooling value (heat loss) of 8 kW/m^2 was estimated using the dish temperature and assuming thermal equilibrium existed at the end of each test. Only a few data points were influenced by this correction. At higher mass loss rates, the vapor layer provided sufficient shielding to minimize this cooling effect. A more detailed discussion of this correction is given elsewhere.[15]

Global heat of gasification

In the process of developing the experimental method for these tests, several additional noteworthy complications were encountered that affected the measurement of the mass loss rates and the calculation of the global heat of gasification. A significant complication involved the condensation of fluid vapor on the sample support hardware, primarily for the low viscosity fluids. For the high viscosity fluids, condensation on the sample support hardware was typically not a problem due to their lower mass loss rates. An additional problem is that of trace catalyst effects on siloxanes at high temperature; trace catalyst residues are present in all siloxanes and their influence can only be minimized. Careful attention to cleaning and handling of dishes and fluids is essential to minimize the addition of troublesome contaminants.

Despite these experimental sensitivities, experiments conducted under the same experimental conditions in this study were remarkably repeatable and consistent. The methods used to correct for these sensitivities are believed to have produced reliable measurements of the mass loss rate from which reliable values for the global heat of gasification were obtained.

Using the above estimates of the various heat losses, global heat of gasification values were calculated using the measured average mass loss rates. The mass loss rate data are summarized in Figs 9 (pure fluids) and 10 (broad distribution fluids). The global heat of gasification is derived from the inverse of the slope and a significant correction for surface reradiation is required [see Fig. 12] for the intermediate and high visocity fluids. The values from all of the experiments with a particular fluid were then averaged to obtain an average global heat of gasification value. The measured global heat of gasification values for the eight PDMS-200 fluids are summarized in Fig. 13. Figure 13 also shows a graphical comparison of the measured and calculated values of the global heat of gasification for the low viscosity fluids. The calculated values are based on the heat capacity and heat of vaporization values for each of these oligomers. The volatiles identified and quantified in this investigation[13] confirm that these oligomers are gasified intact with no molecular degradation/rearrangement evident. The good agreement between the measured and calculated values for these low viscosity fluids supports the overall experimental approach used in this investigation. The 5 cS fluid consists of a mixture of various linear species and its

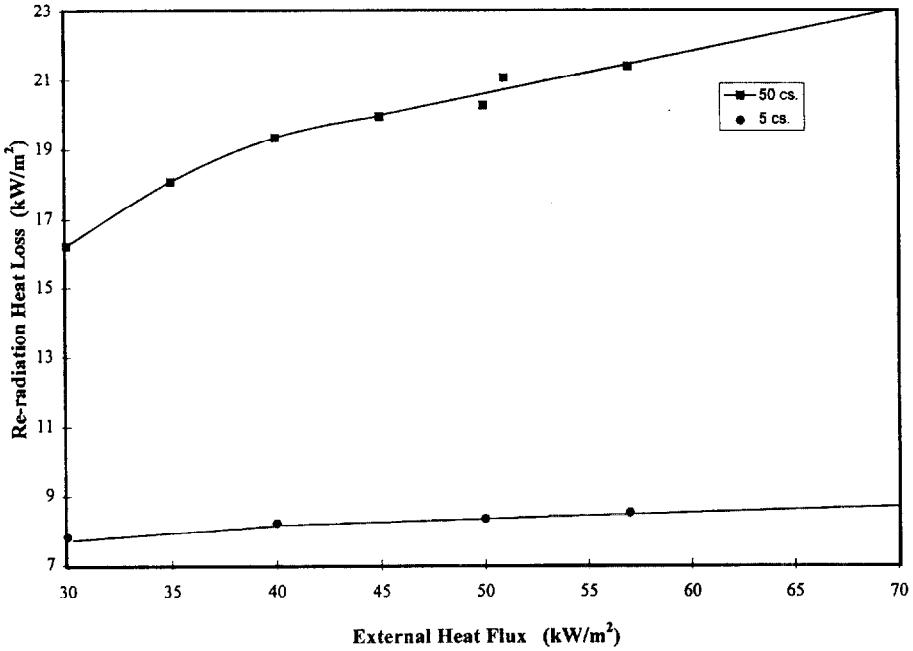

Figure 12. Re-radiation heat loss flux from the test sample as a function of external radiant flux for 5 cS and 50 cS PDMS fluids.

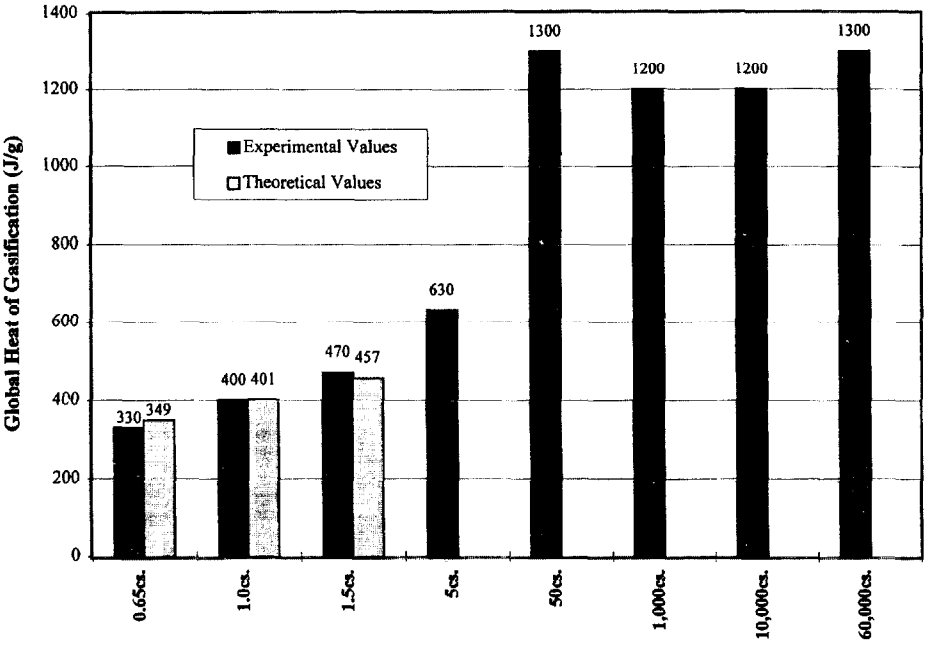

Figure 13. Global heat of gasification va1lues for PDMS oligomers and fluids.

calculated global heat of gasification is not uniquely defined. However, the measured global heat of gasification (630 kJ/kg) is in good agreement with those of its major components ($MD_{6,7,8,9}M$).

The 50 cS fluid and high viscosity fluids all had similar global heat of gasification values in the range of 1200 to 1300 kJ/kg. This is attributed to their similar structure and gasification behavior (Ref. 13 [Table 3]). Except for the 50 cS fluid, the dominant gasification route for these fluids after the initial ~ 10% of mass loss is that of thermal induced degradation/rearrangement to short chain cyclic oligomers along with a wide range of intermediate chain length cyclic dimethylsiloxanes. The gasification of the 50 cS occurs via a combination of two routes: volatilization and thermal induced degradation. Furthermore, the similarity between the heat of gasification values for the 50 cS and high viscosity fluids suggests that both the distillation and pyrolysis processes for these higher viscosity fluids require similar amounts of energy. The overall pyrolysis rate of this fluid parallels that of the higher viscosity fluids and this is perhaps fortuitous.

The influence of trace catalyst residues on the thermal stability of PDMS polymers is well known. In commericial materials based on PDMS, this issue is addressed by careful removal of potentially catalytic materials or by the addition of appropriate stabilizers. The influence of trace catalytic residues on their gasification behavior was briefly investigated. The mass loss rate data for a variety of PDMS polymers are given in Fig. 14. The pyrolysis rate data for commercial-grade silicone fluids are represented by the solid curve (from Fig. 10). The 60K-FC data points represent pyrolysis rate data for three commerical-grade fluids (60 000 cS) produced using a catalyst system designed for the easy removal of catalyst residues. The similarity of their pyrolysis behavior to other commercial-grade fluids is expected. Fluids A, B, and C (60 000 cS) contain known catalyst residues in the parts per million range (< 50 ppm, [w/w]). The fluids (TAY-1, TAY-2) are ultra-clean as a result of exhaustive purification efforts. Note their significantly lower pyrolysis rates. The calculation of a heat of gasification for these ultra-clean fluids results in a value of ~ 3000 kJ/kg. Since the dominant pyrolysis process is that of cyclic formation via siloxane bond scission, it is of some interest to compare this measured heat of gasification to other measurements of Arrhenius activation energy for the pyrolysis of PDMS.

Thomas and Kendrick[17] using isothermal TGA measured an Arrhenius activation energy of 43 kcal/mole) (180 kJ/mole) for PDMS. More recently, Zeldin *et al.*,[10] using isothermal degradation methods and measuring the rates of depolymerization of specially prepared 'catalyst free' polymers, measured an activation energy of 80 kcal/mole (335 kJ/mole) which was in fair agreement with the Si–O bond energy of 108 kcal/mole (452 kJ/mole).[18] In these investigations, discrepancies between the measured activation energies and the siloxane bond energy were attributed to either the presence of trace catalysts or specific details of the polymer degradation mechanism were inferred.

Our measured global heat of gasification of ~ 3000 kJ/kg results in an estimated energy of ~ 2400 kJ/kg (180 kJ/mole) for overall siloxane bond rearrangement, i.e. ~ 600 kJ/kg is associated with heat capacity requirements. This is in fair agreement with the results of Thomas and Kendrick. The general agreement amongst the measured activation energies derived via these different thermolysis protocols suggests that the energy associated with siloxane bond scission is a major factor in determining the gasification rates of these polymers and ultimately their burning rates. These findings also highlight the significant role which the presence of

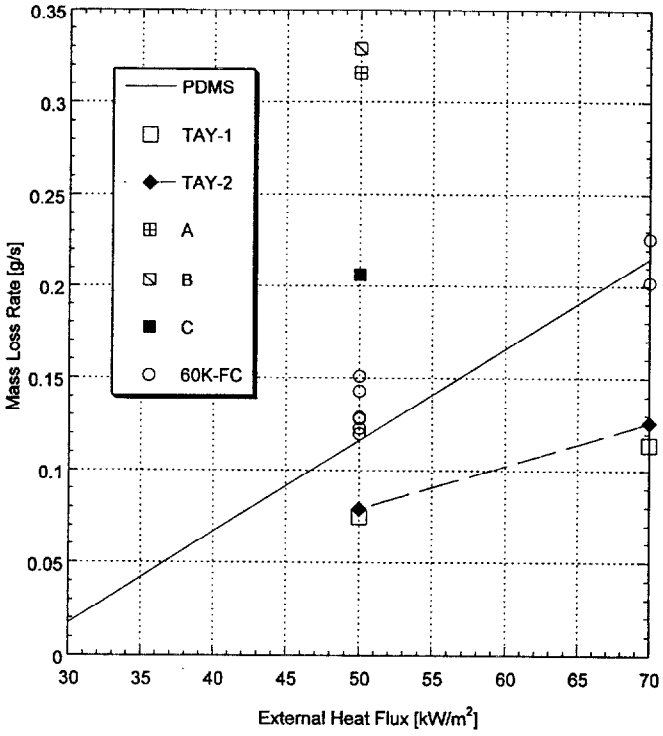

Figure 14. Effect of residual catalysts: average mass loss rates as a function of radiant flux for various PDMS polymers.

potentially catalytic species may exert on the pyrolysis behavior (burn behaviour) of PDMS. These polymers are typically utilized in formulated products containing fillers, additives, curing agents, pigments, etc. Consequently, the pyrolysis behavior of formulated products may differ appreciably despite their containing the same primary component, i.e. high viscosity PDMS polymer.

CONCLUSIONS

The gasification apparatus used in this investigation provides a unique capability for measuring a key fire behavior parameter (global heat of gasification) for materials. The apparatus simulates the pyrolysis conditions in a diffusion-controlled fire scenario. Mass loss, material temperatures, visual observation and video data provide excellent documentation of the pyrolysis process.

The measurement of reliable global heats of gasification require substantial corrections for: (1) the absorption (attenuation) of incident radiant flux by vapor when pyrolyzing volatile low molecular weight fluids, and (2) the re-radiation of energy from the sample surface for those materials which pyrolyze at relatively high temperatures (high molecular weight or high viscosity dimethylsiloxane fluids). This results in a significantly reduced heat flux to the surface to drive the pyrolysis process. Other effects such as heat sink and loss of heat through the sample container and convective heat loss from the sample surface were noted to be far less significant.

The average gasification rate of each dimethylsiloxane fluid increased linearly with increasing external radiant flux. The global heat of gasification of dimethylsiloxane oligomers increases with their molecular weight. These molecular species volatilize intact whereas longer chain length materials thermally degrade via siloxane bond rearrangement to form volatile oligomers. For all higher molecular weight dimethylsiloxanes ($\eta \geqslant 50$ cS fluid), the global heat of gasification is relatively constant at 1200 to 1300 kJ/kg. The high temperature pyrolysis ($\geqslant 400°C$) of dimethylsiloxanes is sensitive to trace level residual catalytic materials. The global heat of gasification of ultra-clean fluids was substantially higher (~ 3000 kJ/kg) and in generally good agreement with other thermal measurements and calculated energy requirements for gasification.

Acknowledgements

This work was conducted under a CRADA between NIST and Dow Corning Corporation. We would like to acknowledge the technical assistance of Mr. Ken Steckler and Dr. Steve Ritchie of BFRL/NIST.

REFERENCES

1. R. R. Buch, Rates of heat release and related fire parameters for silicones, *Fire Safety Journal* **71**, 1 (1991).
2. R. A. Hemstreet, *Flammability Tests of Askarel Replacement Transformer Fluids*, National Electrical Manufacturers Association, 2102 L Street N.W., Suite 300, Washington, D.C. 20037, FMRC Serial No. 1A7R3.RC, FMRC No. RC78-T-43, August, 1978.
3. M. Kanakia, Characterization of transformer fluid pool fires by heat release rate calorimetry. Southwest Research Institute, Project No. 03-5344-001, Presented at the *4th Int. Conf. Fire Safety, Univ. of San Francisco*, 1979.
4. A. Tewarson, J. L. Lee and R. F. Pion, *Fire Behavior of Transformer Dielectric Insulating Fluids*, prepared for US Department of Transportation, Kendall Square, Cambridge, MA 02142, Report FRA/ORD-80/08, January, 1980.
5. R. R. Buch, A. Hamins,. K. Konishi, D. Mattingly and T. Kashiwagi, Radiative emission fraction of pool fires burning silicone fluids. *Comb. Flame* **108**, 118–126 (1997).
6. J. Lipowitz, Flammability of polydimethylsiloxanes. 1. A model for combustion. *J. Fire Flamm.* **7**, 482 (1976).
7. J. Lipowitz and M. J. Ziemelis, Flammability of polydimethylsiloxanes. 2. Flammability and fire hazard properties. *J. Fire Flamm.* **7**, 504 (1976).
8. O. K. Johannson and C. L. Lee, Cyclic siloxanes and silazanes. In *High Polymers*, Chapter 6, ed. by H. C. Frisch, Volume XXVI, Wiley-Interscience, New York (1972).
9. N. Grassie and I. G. Macfarlane, The thermal degradation of polysiloxanes, I. Poly(dimethylsiloxane), *Eur. Pol. J.* **14**, 875–884 (1978).
10. M. Zeldin, D. W. Kang, G. P. Rajendran, B. Qian and S. J. Choi, Kinetics of thermal depolymerization of trimethylsiloxy end-blocked polydimethylsiloxane and polydimethysiloxane-*N*-phenylsilazane copolymer. *Sci. Total Environ.* **73**, 71–85 (1988).
11. *Siloxane Polymers*, ed. by S. J. Clarson and J. A. Semlyen, Chapters 3 and 5, P T R Prentice-Hall (1993).
12. J. Steciak and A. Tewarson, *Flammability Characteristics of Dielectric Insulating Fluids and Resins*, prepared for Dow Corning Corporation, Midland MI, Report No. FMRC J.I.0M2R2.RC, April, 1992.
13. R. R. Buch, P. J. Austin and T. Kashiwagi, Gasification of silicone fluids under external thermal radiation — Part 2. Characterization and quantitation of gasification products, *Fire Mater.* **22**, (1998).
14. T. E. Daubert and R. P. Danner, *Physical and Thermodynamic Properties of Pure Chemicals (Design Institute for Physical Property Research, DIPPR, Data Compilation)*, Taylor & Francis, Bristol, PA (1995).
15. P. J. Austin, R. R. Buch and T. Kashiwagi, *Gasification of Silicone Fluids under External Thermal Radiation* NISTIR 6041, U.S. Department of Commerce, July 1997.
16. T. Kashiwagi, A. Omori and H. Nanbu, Effects of melt viscosity and thermal stability on polymer gasification, *Comb. Flame* **81**, 188–201 (1990).
17. T. H. Thomas and T. C. Kendrick, Thermal analysis of polydimethylsiloxanes. Part I. J. Polym. Sci. Part A-2,(7) 537 (1969).
18. T. L. Cottrell, *The Strenths of Chemical Bonds*, 2nd Edn, p-250. Butterworths London (1958).